*Manuscript
Click here to view linked References

Bioactive Carbon–PEEK Composites Prepared by Chemical Surface Treatment

Toshiki Miyazaki[1], Chisato Matsunami[1] and Yuki Shirosaki[2]

[1]Graduate School of Life Science and Systems Engineering, Kyushu Institute of Technology, Japan

[2]Frontier Research Academy for Young Researchers, Kyushu Institute of Technology, Japan

Corresponding author:

Toshiki Miyazaki

Graduate School of Life Science and Systems Engineering, Kyushu Institute of Technology, 2-4, Hibikino, Wakamatsu-ku, Kitakyushu 808-0196, Japan

Tel/Fax: +81-93-695-6025

E-mail: tmiya@life.kyutech.ac.jp

© 2016. This manuscript version is made available under the CC-BY-NC-ND 4.0 license
http://creativecommons.org/licenses/by-nc-nd/4.0/

Abstract

Polyetheretherketone (PEEK) has attracted much attention as an artificial intervertebral spacer for spinal reconstruction. Furthermore, PEEK plastic reinforced with carbon fiber has twice the bending strength of pure PEEK. However, the PEEK-based materials do not show ability for direct bone bonding, i.e., bioactivity. Although several trials have been conducted for enabling PEEK with bioactivity, few studies have reported on bioactive surface modification of carbon–PEEK composites. In the present study, we attempted the preparation of bioactive carbon-PEEK composites by chemical treatments with H_2SO_4 and $CaCl_2$. Bioactivity was evaluated by *in vitro* apatite formation in simulated body fluid (SBF). The apatite formation on the carbon–PEEK composite was compared with that of pure PEEK. Both pure PEEK and carbon-PEEK composite formed the apatite in SBF when they were treated with H_2SO_4 and $CaCl_2$; the latter showed higher apatite-forming ability than the former. It is conjectured that many functional groups able to induce the apatite nucleation, such as sulfo and carboxyl groups, are incorporated into the dispersed carbon phase in the carbon–PEEK composites.

Keywords

Polyetheretherketone (PEEK), carbon–PEEKcomposite, Apatite, Bioactivity, Simulated body fluid (SBF), Surface modification

1 Introduction

Spinal diseases such as disk herniation, spinal stenosis and compression fracture cause neuropathic pain [1,2]. In severe cases, implantation of artificial intervertebral spacers is needed. Titanium and its alloys, carbon and polyetheretherketone (PEEK) are used for this purpose. In particular, PEEK has attracted much attention, as it reduces stress shielding by having a lower elastic modulus than metallic biomaterials [3]. PEEK plastic reinforced with carbon fiber has a bending strength twice as high as pure PEEK [4] and is expected to become a novel biomaterial for spinal reconstruction. Although elastic modulus of carbon-PEEK is higher than that of pure PEEK, it is analogous to that of human cortical bone with carbon content less than 30%. Nonetheless, neither PEEK nor PEEK reinforced with carbon fiber show ability for direct bone bonding. Thus, autograft implantation around the spinal devices is needed for bone fixation in bone tissue. Additional surgery is needed to extract the autograft, which subjects the patient to severe physical strain. Therefore, tight bone integration of PEEK medical devices is necessary for long-term stability *in vivo* and improvement of patients' quality of life.

It is reported that an essential requirement for artificial materials to exhibit bioactivity is the formation of bone-like apatite on their surfaces in the body environment through chemical reaction with body fluid [5]. The apatite formation can be reproduced in simulated body fluid (SBF) with inorganic ion concentrations similar to human extracellular fluid [6]. The development of bioactive PEEK has been attempted by several techniques [7]. For example, sulfuric acid treatment [8], sol-gel titania coating [9], PEEK–hydroxyapatite composite [10-12] and composite of PEEK and sol-gel-derived $CaO\text{-}SiO_2$ powder [13] have been proposed. Main technique of bioactive PEEK preparation is mixing PEEK with bioactive ceramic particles. However, only a part of the added ceramics is exposed to body fluid to contribute to their bioactivity. So large amount of the ceramic addition is needed for achieving bone bonding. The composite with high ceramic content is liable to be brittle. Ha *et al.* also prepared a bioactive carbon–PEEK composite by Ti coating via vacuum plasma spraying and subsequent NaOH treatment [14]. In this case, a sodium titanate layer formed by the NaOH treatment contributed to the apatite formation. However, no other studies have been proposed on the bioactivity of the carbon–PEEK composite. In

particular, using a surface modification to provide the composite itself with apatite-forming ability has not been suggested.

In the present study, we carried out chemical treatments of the carbon–PEEK composite with sulfuric acid and calcium salt solution. Subsequently, *in vitro* apatite-forming ability was evaluated in SBF. The effect of carbon incorporation into PEEK plastics on the apatite formation is discussed. It is assumed that functional group able to induce the apatite formation well incorporated on the composites, since carbon has higher reactivity than PEEK. Actually, surface modification of the carbon by carboxyl group [15] and sulfo group [16] has been reported.

2 Materials and Methods

Disks of the pure PEEK (Victrex plc, UK) and carbon-PEEK composite containing 30% by mass of carbon fiber (diameter of 10 mm, thickness of 1.2 mm; Sumitomo Chemical Co., Japan), and rectangular pure carbon substrates (10 × 10 × 1 mm; Nilaco Co., Japan) were soaked in 5 mL of concentrated sulfuric acid (97 wt%) at 20 °C for 10 min, and then soaked in ultrapure water for 10 min and dried at 60 °C for

30 min. After the treatment, they were soaked in 30 mL of 1 M-$CaCl_2$ solution at 36.5 °C for 24 hr. SBF (Na^+ 142.0, K^+ 5.0, Mg^{2+} 1.5, Ca^{2+} 2.5, Cl^- 147.8, HCO_3^- 4.2, HPO_4^{2-} 1.0, SO_4^{2-} 0.5 mM) was prepared by the sequential addition of NaCl, $NaHCO_3$, KCl, $K_2HPO_4 \cdot 3H_2O$, $MgCl_2 \cdot 6H_2O$, $CaCl_2$ and Na_2SO_4 (Nacalai Tesque Inc., Kyoto, Japan) to ultra-pure water according to the previous literature [6]. The pH of the resulting solution was adjusted to 7.4 by the addition of tris(hydroxymethyl)aminomethane (Nacalai Tesque Inc.) and the appropriate volume of a 1 M-HCl solution. The samples were then soaked in 30 mL of SBF at 36.5 °C for 14 days.

The chemical structures of the samples were analyzed by Fourier transform infrared spectroscopy (FT-IR; FT/IR-6100, JASCO Co., Tokyo, Japan) using an attenuated total reflectance method. The scan range for the FT-IR analysis was set from 400 to 4000 cm^{-1} at a resolution of 4 cm^{-1}. The surface morphology and elemental composition were characterized by energy dispersive X-ray (EDX) analysis using an EMAX Energy system (Horiba Ltd., Japan) equipped with a scanning electron microscope (SEM; S-3500N; Hitachi Co., Japan).

The crystalline structure of the samples was characterized by thin-film X-ray diffraction (TF-XRD; MXP3V, Mac Science, Co., Yokohama, Japan). Monochromated Cu-Kα radiation was used for the TF-XRD analysis, which was fixed at 1° against the surface of each specimen with a scan rate of $0.02°\cdot sec^{-1}$. The coverage ratio of the apatite precipitate formed on the substrates in SBF was determined from SEM photographs using ImageJ software. The amount of Ca^{2+} incorporated into the substrates by $CaCl_2$ treatment was determined by soaking in ultrapure water at room temperature for 24 hr and measuring the Ca^{2+} concentration of the water by ion/pH meter (F-23IIC, Horiba Ltd.). Contact angle of the specimens before and after H_2SO_4 treatment was measured by a contact angle meter (DMe-200, Kyowa Interface Science Co., Ltd., Saitama, Japan). One sample was used for one condition except measurement of contact angle and coverage ratio of the apatite.

3 Results and Discussion

Figure 1 shows water contact angle of the substrates before and after H_2SO_4 treatment. The contact angle was significantly decreased for all the substrates after the

treatment. This means that H_2SO_4 treatment is quite effective for making PEEK and carbon more hydrophilic.

Figure 2 shows EDX spectra of the surfaces of pure PEEK and carbon-PEEK composites subjected to H_2SO_4 treatment. Peaks of S are observed for both specimens. This suggests that the sulfo group is incorporated into both the substrates.

Figure 3 shows SEM photographs of the surfaces of pure PEEK and carbon-PEEK composites subjected to H_2SO_4 and $CaCl_2$ treatments. Needle-like particles were partially observed on the treated surfaces. The present results indicate that calcium sulfate may be precipitated on the treated specimens, since the typical calcium sulfate crystal takes needle-like structure.

The coverage ratios of the apatite particle on pure PEEK and carbon–PEEK calculated from SEM photographs were 6.59±7.33% and 64.6±14.0%, respectively (N=10). The amount of Ca^{2+} incorporated into pure PEEK and carbon–PEEK by $CaCl_2$ treatment was 2.1±0.9 and 3.6±0.3 μmol/substrate, respectively. This means that carbon–PEEK has significantly higher ability of the apatite formation in SBF than pure PEEK even after the same chemical treatments.

Figure 4 shows TF-XRD patterns of the surfaces of pure PEEK and carbon–PEEK composites subjected to H_2SO_4 and $CaCl_2$ treatments. Peaks assigned to $CaSO_4 \cdot 2H_2O$ (JCPDS#33-0311) were observed for both substrates after the treatment. The peaks at 20.7, 23.4, 29.1, 31.1, 33.3° were due to $\bar{1}21$, 040, $\bar{1}41$, 121 and 051 diffraction of $CaSO_4 \cdot 2H_2O$, respectively [17]. This indicates that the deposited needle-like particles are $CaSO_4 \cdot 2H_2O$.

Figure 5 shows SEM photographs of the surfaces of pure PEEK and carbon-PEEK composites subjected to H_2SO_4 and $CaCl_2$ treatments, which were soaked in SBF for 14 days. Spherical particles were partially observed on pure PEEK, while the surface of carbon–PEEK substrates were almost covered with fine particles. Ca/P molar ratio of the deposits was 1.42 for both the specimens. This result coincides with characteristic of bone mineral and bone-like apatite with Ca deficiency.

Figure 6 shows TF-XRD patterns of the surfaces of pure PEEK and carbon–PEEK composites subjected to H_2SO_4 and $CaCl_2$ treatments, which were soaked in SBF for 14 days. Peaks assigned to low-crystalline apatite (JCPDS #09-0432) were observed at 26 and 32°. The peak at 26° is due to 002 diffraction of apatite while a broader peak at

about 32° is an envelope of 211, 112 and 300 diffractions of apatite [16]. Peak intensity of the carbon–PEEK composite was higher than that of pure PEEK. These results also support higher apatite-forming ability of the carbon–PEEK composites.

Figure 7 shows FT-IR ATR spectra of the surfaces of pure carbon substrates subjected to H_2SO_4 treatment. Peaks assigned to O=S=O were observed at 1050 and 1200 cm^{-1}, while that assigned to C=O was observed at 1650 cm^{-1} [16]. This means that sulfo group can be incorporated even on pure carbon by H_2SO_4 treatment.

Figure 8 shows SEM photographs of the surfaces of pure carbon substrates subjected to H_2SO_4 and $CaCl_2$ treatment, which were soaked in SBF for 14 days. Deposits were observed on the specimens after soaking in SBF. They were confirmed to contain Ca and P by EDX. This indicates that H_2SO_4-treated pure carbon has ability to form a calcium phosphate in SBF, although it was not confirmed with the apatite.

The hydrophilic sulfo group was incorporated into both the pure PEEK and carbon–PEEK composites by H_2SO_4 treatment. This is supported by the significant improvement of hydrophilicity shown in Fig. 1. Judging from the result that the incorporated sulfo group was converted to calcium sulfate dihydrate by the subsequent

$CaCl_2$ treatment, it was eliminated from the PEEK chain. The sulfonation reaction of the aromatic ring is represented as follows [18]:

$$C_6H_6 + H_2SO_4 \rightleftarrows C_6H_5SO_3H + H_2O \qquad (1)$$

On the other hand, desulfonation occurs as a reverse reaction in aqueous conditions. The eliminated sulfo group may react with Ca^{2+} to form the calcium sulfate dihydrate, which has the lowest solubility in water among various calcium sulfates [19]. The release of the calcium sulfate would induce the apatite formation by increasing the supersaturation degree of the surrounding SBF with respect to the apatite.

The present results indicate that both pure PEEK and carbon–PEEK composites can form the apatite in SBF when they are treated with H_2SO_4 and $CaCl_2$ solutions. The carbon–PEEK composites showed significantly higher ability for apatite formation than pure PEEK (Figs. 5 and 6). It is assumed that many functional groups able to induce apatite nucleation are incorporated into the dispersed carbon phase in the carbon–PEEK composites. This assumption is supported by the results that even pure carbon can be

incorporated into the sulfo group and carboxyl group by H_2SO_4 treatment (Fig. 6), and that the treated carbon forms calcium phosphate in SBF (Figs. 7 and 8). Both the sulfo group and the carboxyl group have the ability for apatite formation in the body environment [20–22]. Furthermore, carbon–PEEK composites contained larger amounts of Ca^{2+} than the pure PEEK by $CaCl_2$ treatment. Actually, Ca concentration of SBF was 2.7 and 3.7 mM after soaking of pure PEEK and carbon-PEEK, respectively, for 7 days (Original SBF: 2.5 mM). The ionic activity product (*IP*) of the hydroxyapatite was estimated according to equation (2) and using Ca^{2+} and PO_4^{3-} concentrations, and pH of SBF.

$$IP = (g_{Ca^{2+}})^{10}(g_{PO_4^{3-}})^{6}(g_{OH^-})^{2}[Ca^{2+}]^{10}[PO_4^{3-}]^{6}[OH^-]^{2} \quad (2)$$

The ionic activity coefficient value of $\gamma_{Ca^{2+}}$, $\gamma_{PO_4^{3-}}$ and g_{OH^-} are supposed to be 0.36, 0.06 and 0.72 at physiological ionic strength (μ=0.16) [23]. The pH of SBF after soaking of both the specimens for 7 days was almost the same (7.58). Judging from the result that the carbon-PEEK released larger amount of Ca^{2+} than pure PEEK, the composite would provide higher degree of supersaturation with respect to the

hydroxyapatite. Overall, these factors would contribute to superior apatite formation on the carbon–PEEK composites.

Zhao *et al.* reported that apatite covered almost the entire surface of the specimen after soaking in SBF for 28 days [8]. On the other hand, most of the surface treated with carbon–PEEK composite was covered with the apatite within 14 days. This suggests that surface modification in the present study is effective for acceleration of the apatite formation. However, most of clinically used bioactive materials form the apatite within 1 week [24]. Therefore further acceleration in the apatite formation is needed for medical application in future work. Moreover, adhesion of the apatite layer on the substrates was not so high. This would be attributed to desulfonation from PEEK. Therefore improvement of this point is also needed to proceed to further assessment of biological compatibility such as cell culture.

4 Conclusions

Carbon–PEEK composites were found to show bioactivity by surface chemical modification using H_2SO_4 and $CaCl_2$ solutions. Their bioactivity was significantly higher than that of pure PEEK. It was assumed that many functional groups able to induce apatite nucleation are incorporated into the dispersed carbon phase in the composites. These composites are expected to become novel biomaterials for spinal reconstruction for their bioactivity and high mechanical strength. Furthermore, the present modification process would be effective for the development of bioactive carbon-based materials such as graphene.

References

1. E. Siebert, H. Prüss, R. Klingebiel, V. Failli, K.M. Einhäupl and J.M. Schwab, Lumbar spinal stenosis: syndrome, diagnostics and treatment, Nature Rev. Neurology, 5, (2009) 392-403.
2. L. Dang and Z. Liu, A review of current treatment for lumbar disc herniation in children and adolescents, Eur. Spine J., 19 (2010) 205–214.
3. S. M. Kurtz and J.N. Devine, PEEK Biomaterials in Trauma, Orthopedic, and Spinal Implants, Biomaterials, 28 (2007) 4845–4869.
4. D.F. Williams, A. McNamara, R.M. Turner, Potential of polyetheretherketone (PEEK) and carbon-fibre-reinforced PEEK in medical applications, J. Mater. Sci. Lett., 6 (1987) 188-190.
5. T. Kokubo, H.-M. Kim and M. Kawashita, Novel bioactive materials with different mechanical properties, Biomaterials, 24 (2003) 2161-2175.

6. S.B. Cho, T. Kokubo, K. Nakanishi, N. Soga, C. Ohtsuki, T. Nakamura, T. Kitsugi and T. Yamamuro, Dependence of Apatite Formation on Silica Gel on Its Structure: Effect of Heat Treatment, J. Am. Ceram. Soc., 78 (1995) 1769-1774.
7. R. Ma and T. Tang, Current Strategies to Improve the Bioactivity of PEEK, Int. J. Mol. Sci. 15 (2014) 5426-5445.
8. Y. Zhao, H.M. Wong, W. Wang, P. Li, Z. Xu, E.Y.W. Chong, C.H. Yan, K.W.K. Yeung, P.K. Chu, Cytocompatibility, osseointegration, and bioactivity of three-dimensional porous and nanostructured network on polyetheretherketone, Biomaterials, 34 (2013) 9264–9277.
9. T. Kizuki, T. Matsushita, T. Kokubo, Apatite-forming PEEK with TiO_2 surface layer coating, J. Mater. Sci.: Mater. Med., 26 (2015) Article No.41.
10. M.S. Abu Bakar, P. Cheang, K.A. Khor, Mechanical properties of injection molded hydroxyapatite-polyetheretherketone biocomposites, Composites Sci. Tech., 63 (2003) 421–425.
11. J.P. Fan, C.P. Tsui, C.Y. Tang, C.L. Chow, Influence of interphase layer on the overall elasto-plastic behaviors of HA/PEEK biocomposite, Biomaterials, 25 (2004) 5363–5373.
12. B. Yuan, Y. Chen, H. Lin, Y. Song, X. Yang, H. Tang, E. Xie, T. Hsu, X. Yang, X. Zhu, K. Zhang and X. Zhang, Processing and Properties of Bioactive Surface-Porous PEKK, ACS Biomater. Sci. Eng. 2 (2016) 977–986.
13. I.Y. Kim, A. Sugino, K. Kikuta, C. Ohtsuki and S.B. Cho, Bioactive Composites Consisting of PEEK and Calcium Silicate Powders, J. Biomater. Appl., 24 (2009) 105-118.
14. S.-W. Ha, K.-L. Eckert, E. Wintermantel, H. Gruner, M. Guecheva, H. Vonmont, NaOH treatment of vacuum-plasma-sprayed titanium on carbon fibre-reinforced poly(etheretherketone), J. Mater. Sci. Mater. Med., 8 (1997) 881–886.
15. S. Peng, C. Liu and X. Fan, Surface Modification of Graphene Oxide by Carboxyl-Group: Preparation, Characterization, and Application for Proteins Immobilization, Integrated Ferroelectrics 163 (2015) 42-53.
16. H. Yu, Y. Jin, Z. Li, F. Peng, H. Wang, Synthesis and characterization of sulfonated single-walled carbon nanotubes and their performance as solid acid catalyst, J. Solid State Chem., 181 (2008) 432–438.

17. B. Hansen and S. Kiil, Investigation of Parameters Affecting Gypsum Dewatering Properties in a Wet Flue Gas Desulphurization Pilot Plant, Ind. Eng. Chem. Res., 51 (2012) 10100–10107.
18. L.L. Hench (Ed.), An Introduction to Bioceramics, Second Edition, Imperial College Press, 2013, p. 237.
19. T. W. Graham Solomons, Organic Chemistry, Fifth Edition, Wiley, New York, 1992.
20. K.K. Kelley, W.C. Riddell, J.S. Southard, C.T. Anderson, U.S. Dept. of Interior, Bureau of Mines, Technical paper, No. 625 (1941) 55.
21. T. Miyazaki, C. Ohtsuki, Y. Akioka, M. Tanihara, J. Nakao, Y. Sakaguchi and S. Konagaya, Apatite Deposition on Polyamide Films Containing Carboxyl Group in a Biomimetic Solution, J. Mater. Sci.: Mater. Med., 14 (2003) 569-574.
22. T. Kawai, C. Ohtsuki, M. Kamitakahara, T. Miyazaki, M. Tanihara, Y. Sakaguchi and S. Konagaya, Coating of Apatite Layer on Polyamide Films Containing Sulfonic Groups by Biomimetic Process, Biomaterials, 25 (2004) 4529-4534.
23. T. Kawai, C. Ohtsuki, M. Kamitakahara, M. Tanihara, T. Miyazaki, Y. Sakaguchi and S. Konagaya, A Comparative Study of Apatite Deposition on Polyamide Films containing Different Functional Groups under a Biomimetic Condition, J. Ceram. Soc. Japan, 113 (2005) 588-592.
24. W. Neuman, M. Neuman, The chemical dynamics of bone mineral, University of Chicago Press, Chicago, 1958.
25. T. Kokubo (Ed.), Bioceramics and Their Clinical Applications, Woodhead, Cambridge, 2008.

Figure captions

Fig. 1. Water contact angle of the substrates before and after H_2SO_4 treatment (N=3).

Fig. 2. EDX spectra of the surfaces of pure PEEK and carbon–PEEK composites subjected to H_2SO_4 treatment.

Fig. 3. SEM photographs of the surfaces of pure PEEK and carbon–PEEK composites subjected to H_2SO_4 and $CaCl_2$ treatments.

Fig. 4. TF-XRD patterns on the surfaces of pure PEEK and carbon–PEEK composites subjected to H_2SO_4 and $CaCl_2$ treatments.

Fig. 5. SEM photographs of the surfaces of pure PEEK and carbon–PEEK composites subjected to H_2SO_4 and $CaCl_2$ treatments, which were soaked in SBF for 14 days.

Fig. 6. TF-XRD patterns of the surfaces of pure PEEK and carbon–PEEK composites subjected to H_2SO_4 and $CaCl_2$ treatments, which were soaked in SBF for 14 days.

Fig. 7. FT-IR ATR spectra of the surfaces of pure carbon substrates subjected to H_2SO_4 treatment.

Fig. 8. SEM photograph of the surfaces of pure carbon substrates subjected to H_2SO_4 and $CaCl_2$ treatments, which were soaked in SBF for 14 days.

Figure
Click here to download high resolution image

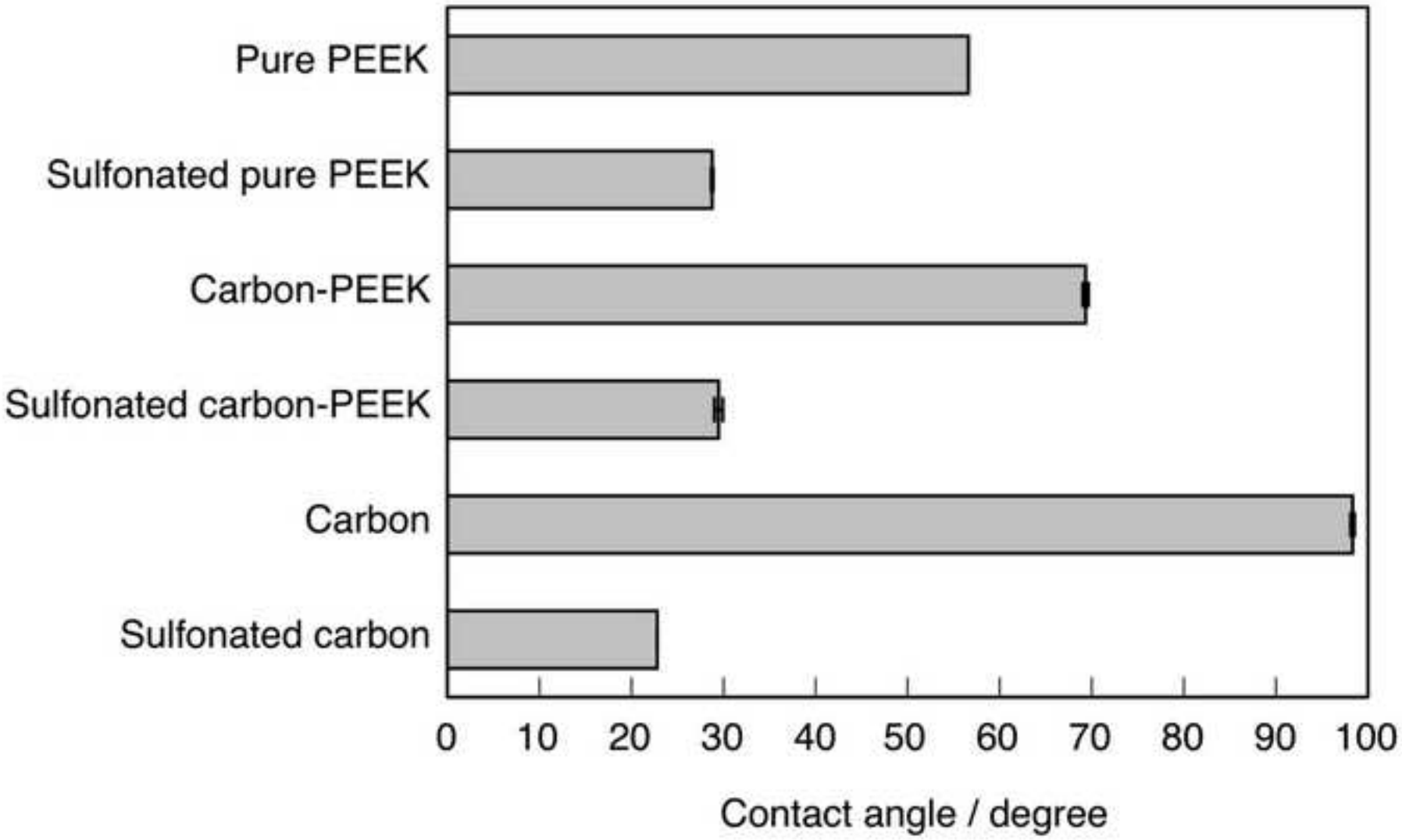

Fig. 1

Figure
Click here to download high resolution image

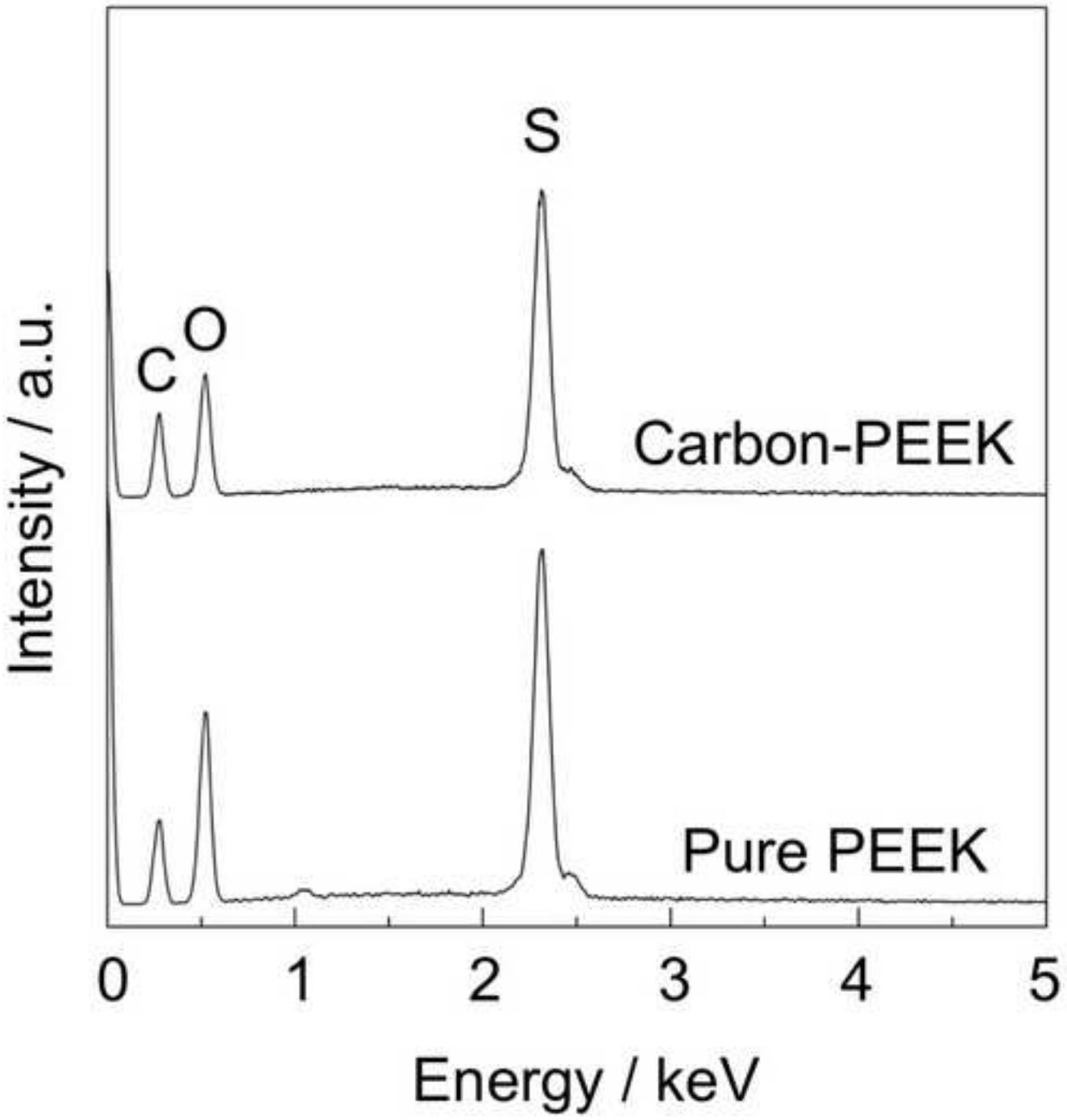

Fig. 2

Figure
Click here to download high resolution image

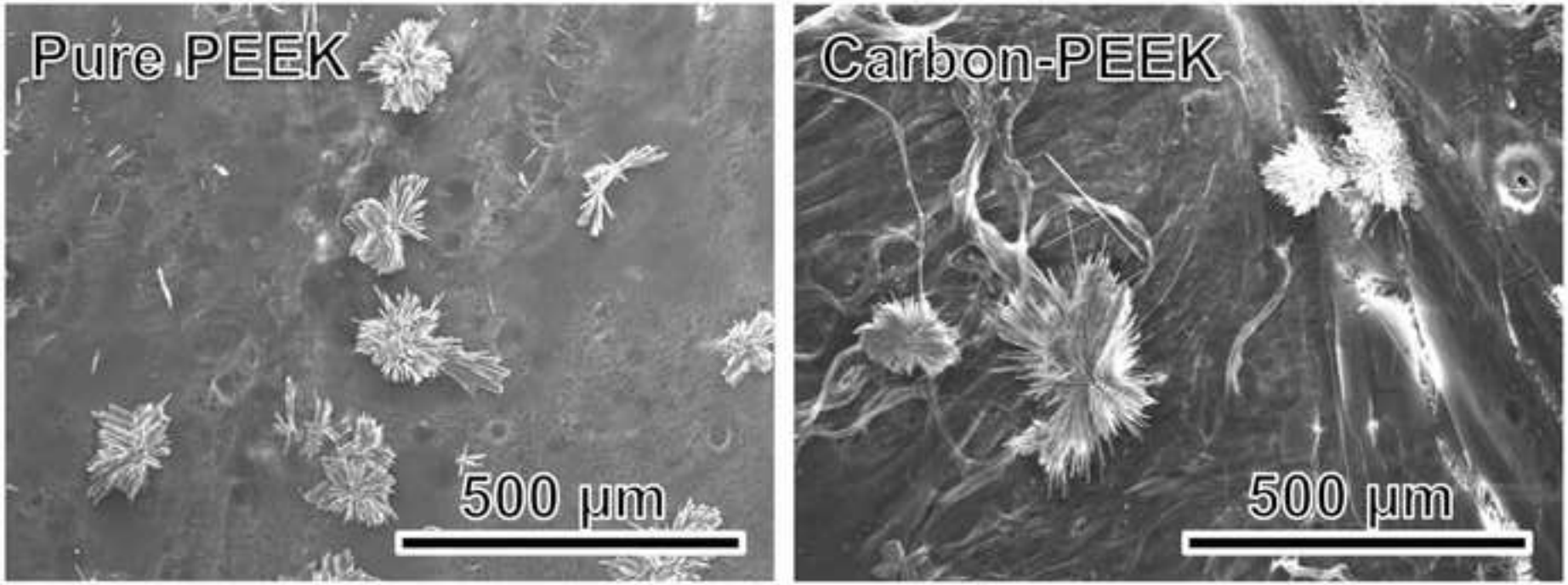

Fig. 3

Figure
Click here to download high resolution image

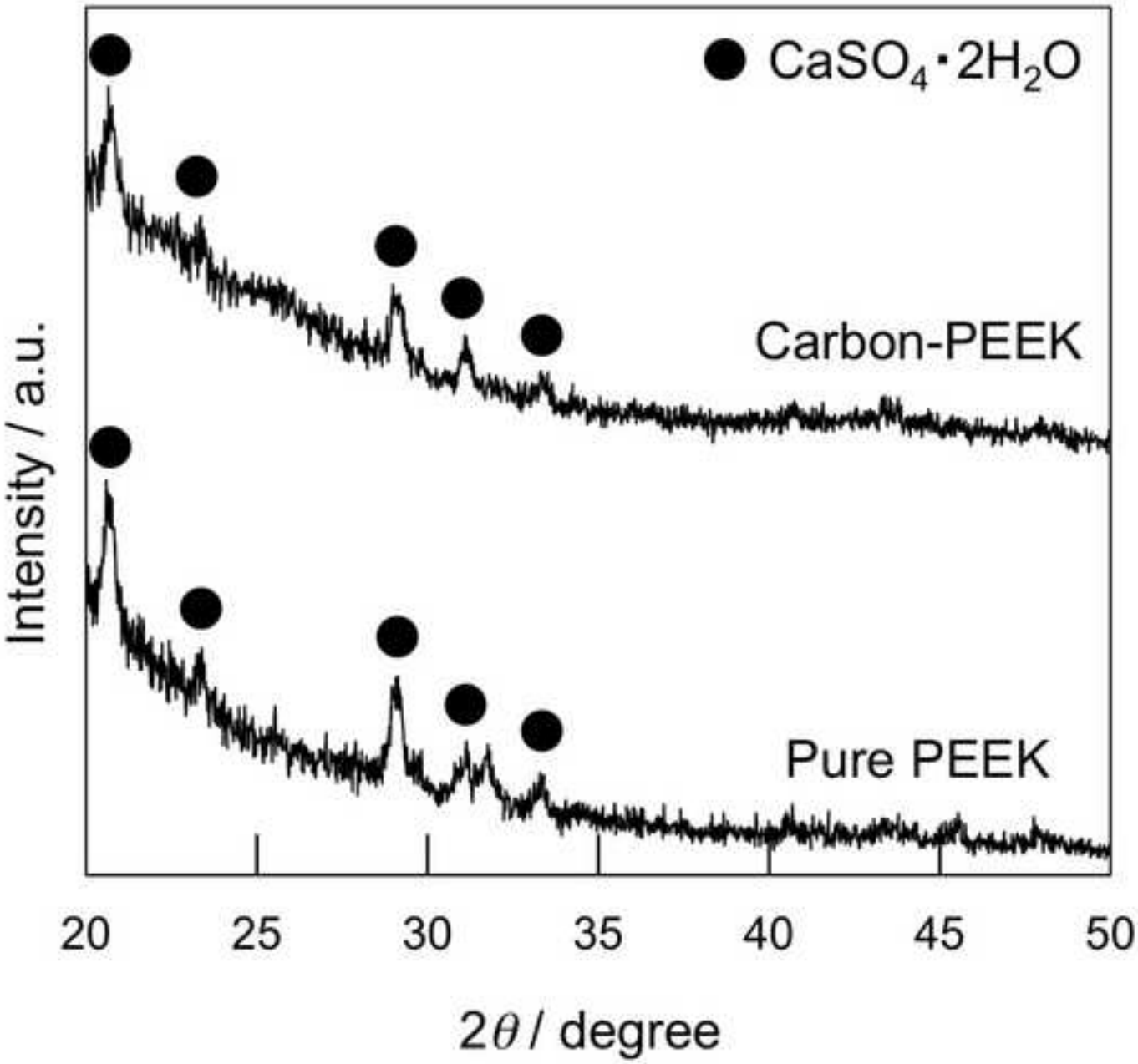

Fig. 4

Figure
Click here to download high resolution image

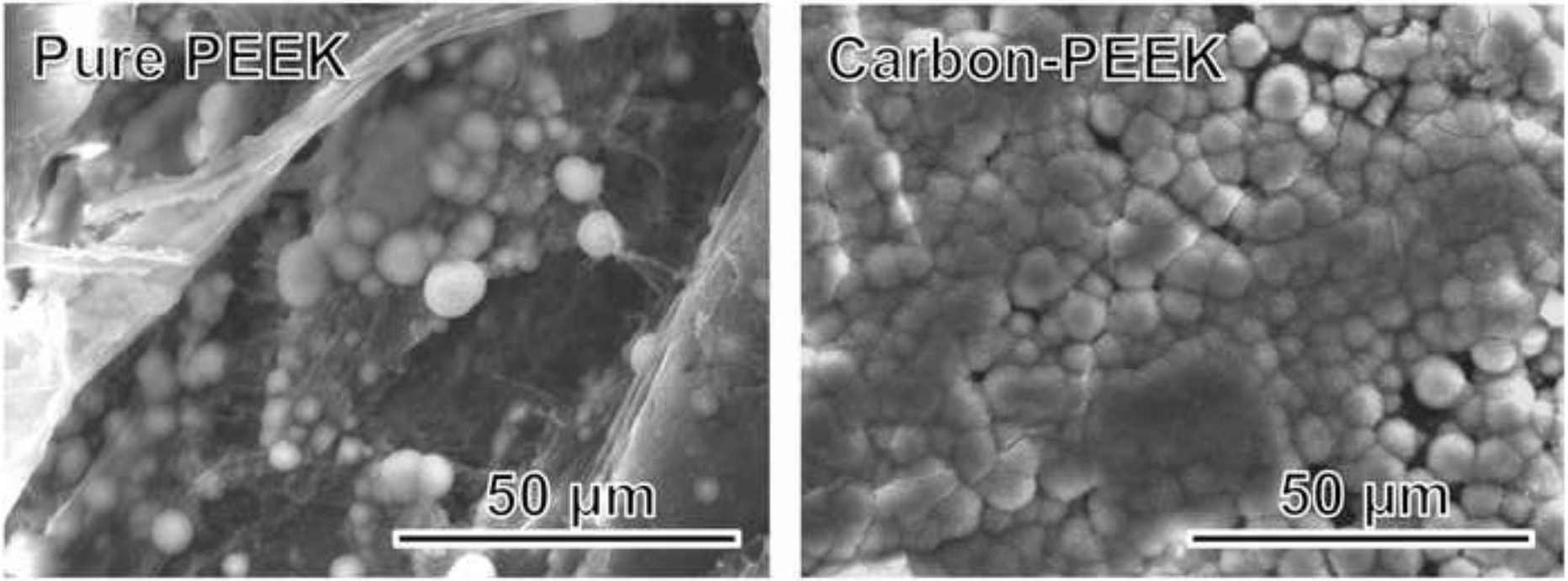

Fig. 5

Figure
Click here to download high resolution image

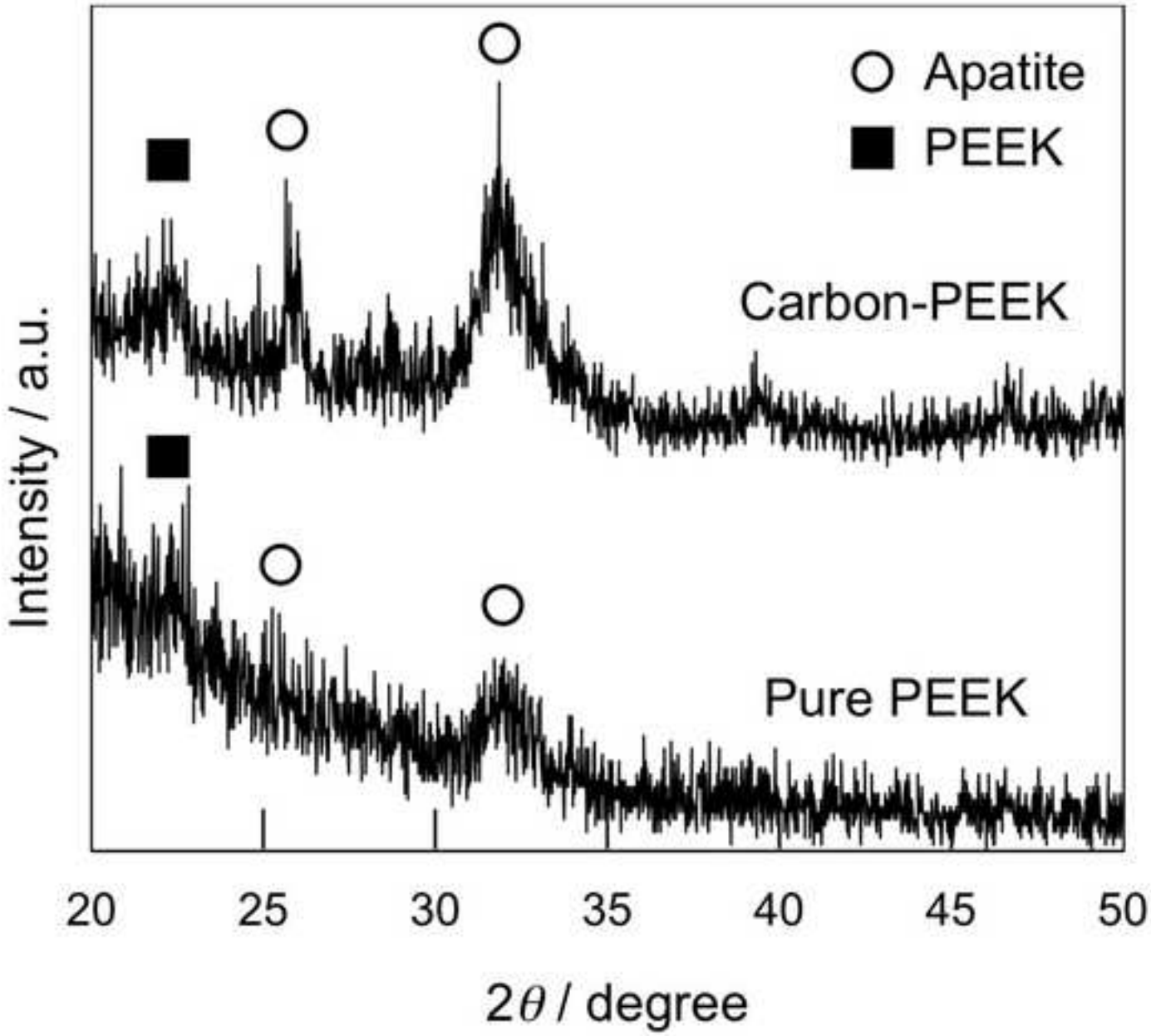

Fig. 6

Figure
Click here to download high resolution image

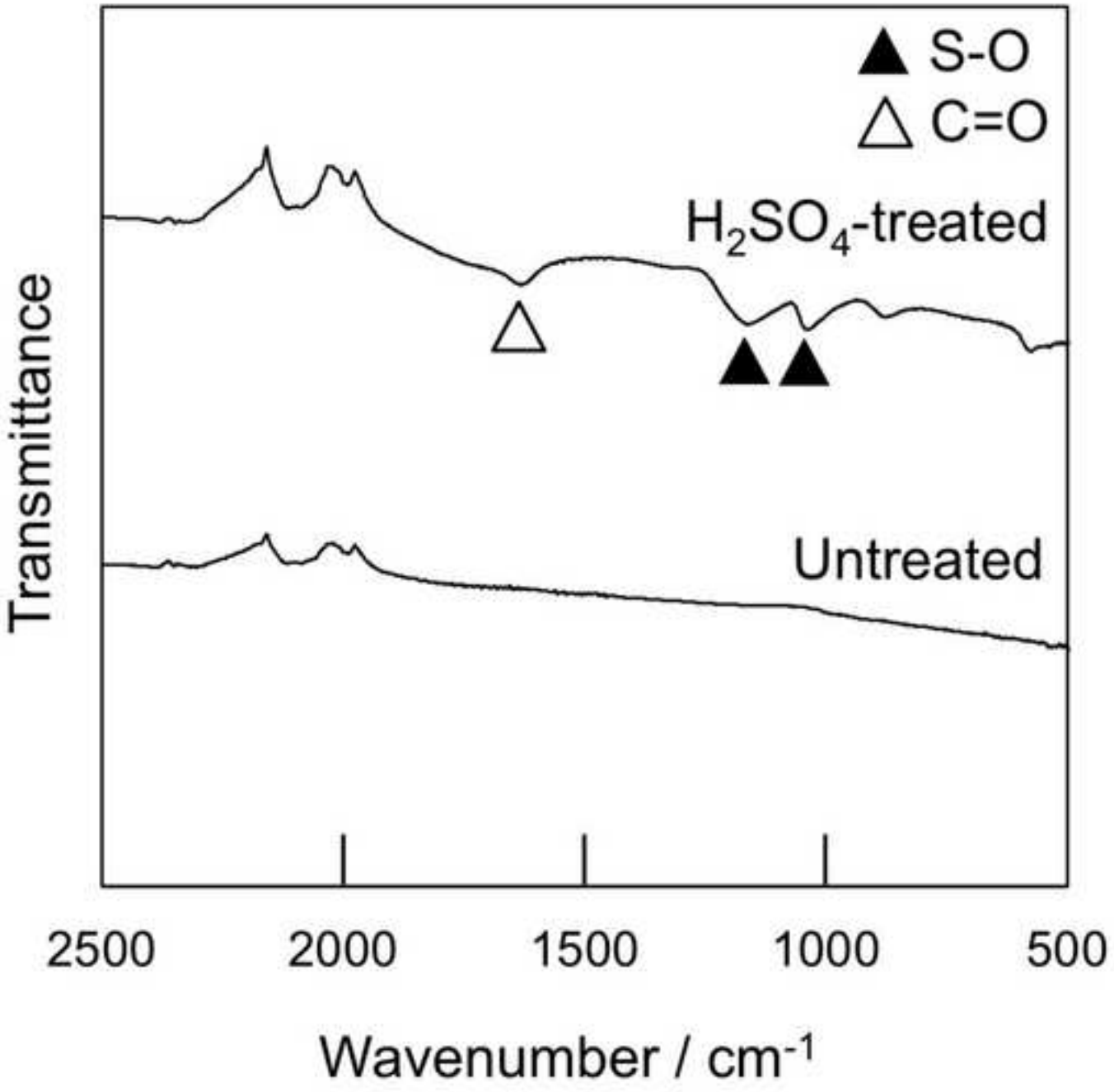

Fig. 7

Figure
Click here to download high resolution image

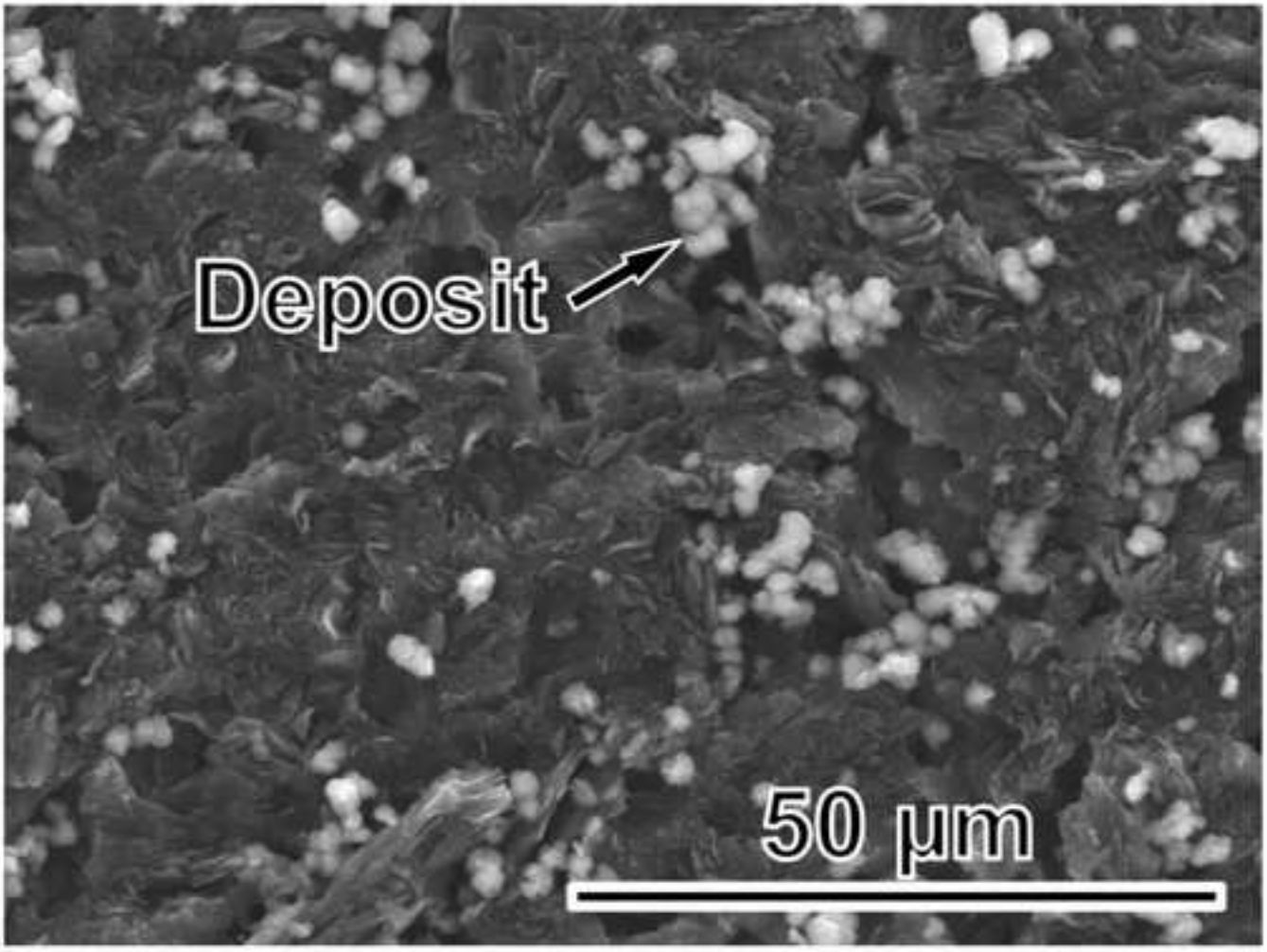

Fig. 8